SENTINEL-1 ASSESSMENT OF THE INTERFEROMETRIC WIDE-SWATH MODE

Pau Prats-Iraola[a], Matteo Nannini[a], Rolf Scheiber[a], Francesco De Zan[a], Steffen Wollstadt[a], Federico Minati[b], Francesco Vecchioli[b], Mario Costantini[b], Sven Borgstrom[c],Prospero De Martino[c], Valeria Siniscalchi[c] , Thomas Walter[d], Michael Foumelis[e], Yves-Louis Desnos[f]

[a] German Aerospace Center (DLR), Germany

[b] e-GEOS SpA, ASI/Telespazio, Italy

[c] National Institute of Geophysics and Volcanology (INGV), Vesuvius Observatory, Italy

[d] German Research Centre for Geosciences (GFZ), Germany

[e] RSAC c/o ESA-ESRIN, EO Science, Applications and Future Technologies Department,Italy

[f] ESA-ESRIN, EO Science, Applications and Future Technologies Department, Italy

ABSTRACT

This contribution reports on the performance investigations of the interferometric wide swath (IW) mode of Sentinel-1, which is implemented using the terrain observation by progressive scans (TOPS) mode. The key aspects of the TOPS mode that need to be considered for accurate interferometric processing will be presented, and first analyses with Sentinel-1 time series will be shown. The results focus on the pilot sites of Campi Flegrei/Vesuvius and Mexico City, as well as Greenland glaciers. Other aspects related to the interferometric performance are also presented, like the burst synchronization, the pointing accuracy, or the considerations when evaluating non-stationary scenes.

Index Terms— Sentinel-1, TOPS Interferometry, coregistration, time series

1. INTRODUCTION

The European Space Agency's (ESA) Sentinel-1A satellite was successfully launched on April 3rd, 2014. Its main operational mode, the Interferometric Wide swath (IW) mode operated as TOPS mode, provides a large swath width of 250 km at a ground resolution of 5×20m in range and azimuth, respectively [1]. Due to the particularities of the acquisition geometry of the TOPS mode, the focusing and interferometric processing of the data needs to consider the special characteristics of the TOPS mode in order to produce interferograms without undesired artifacts.

Section 2 presents first the selected approach for the interferometric processing of Sentinel-1 TOPS data, putting special emphasis on the coregistration and the special considerations for the TOPS mode. Section 3 presents then the main interferometric Sentinel-1 results, which focus on the time series results obtained over Mexico City and Campi Flegrei, and on a particular case of a glacier as a representation of a scenario with a significant azimuthal motion.

2. INTERFEROMETRIC PROCESSING OF TOPS DATA

The interferometric processing of TOPS data requires of special attention due to the azimuth-dependent Doppler variation within a burst, which, similar as in ScanSAR, induces higher coregistration requirements than in the stripmap mode to avoid introducing azimuth phase ramps. For the Sentinel-1 IW mode, the azimuth coregistration shall be accurate within 1 cm to avoid phase jumps larger than 3° between bursts. The selected processing approach is briefly described in Section 2.1, while the special case of non-stationary scenarios is addressed in Section 2.2.

2.1. The TOPS InSAR Chain

Fig. 1 shows the implemented TOPS processing chain. In order to achieve the stringent azimuth coregistraiton requirements, the rationale as presented in [2] is followed. A geometrical approach is very appropriate due to the good accuracy of the restituted and precise Sentinel-1 orbits (≤ 10 cm and ≤ 5 cm accuracy, respectively) together with the small orbital tube (which relaxes the requirements of the external digital elevation (DEM) model). After the computation of the range and azimuth shifts using the nominal approach, it is expected that residual errors in range and azimuth are still present. Especially the offset in azimuth is critical, as a very small offset of few centimeters will introduce an azimuth phase ramp. In a first step, conventional cross-correlation is used to estimate any range or azimuth offset, followed by the enhanced spectral diversity (ESD) approach [2] to refine the estimation of the azimuth offset. This technique exploits the overlap area between bursts to accurately estimate the azimuth offset by

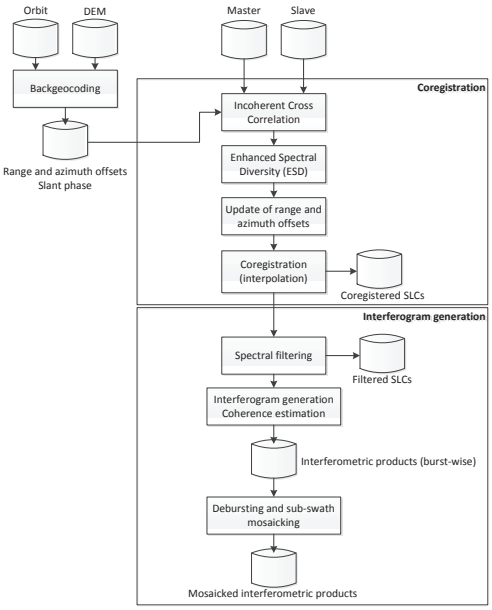

Fig. 1. TOPS Interferometric processing chain.

exploiting the large spectral separation under which the points at the overlap area are observed (see [2] for the details). The proposed workflow is efficient as in the beginning it only processes small blocks to apply cross-correlation and then the overlap areas to apply ESD. Afterwards the range and azimuth matrices are updated and then the complete bursts are interpolated in a burst-wise fashion. The remaining of the processing chain runs as usual, where one can optionally perform the spectral filtering.

2.2. Special Considerations for Non-Stationary Scenes

The InSAR chain described in the previous section is valid for stationary scenarios (i.e., no motion) or scenarios experiencing slow deformation rates (e.g., time series). However, scenarios experiencing large deformations, e.g., glaciers or earthquakes, are challenging due to the phase artifacts that will occur due to the azimuthal motion of the scene. In fact, one should not treat the artifacts as such, since the phase offsets are indeed a legitimate measurement. Indeed, as shown in [3], the phase offset is proportional to the azimuthal motion, namely, $\varphi = 4\pi/\lambda \cdot \Delta x \sin\beta$, being Δx the azimuthal displacement and β the squint angle under which the target has been illuminated. With the maximum squint angles used in the steering of the Sentinel-1 satellite, an azimuthal motion of 10 cm will be sensed by the sensor and introduce a phase offset of about 12° in the interferometric phase. Due to the burst operation (which implies a sudden change in the Doppler centroid at burst edges), phase jumps at burst edges will be visible. In extreme cases, phase jumps larger than $\pm\pi$ can occur, hence complicating the phase unwrapping process between successive bursts. In a generic scenario where no modeling is possible or no a priori deformation is available, it is necessary to perform a data-based approach mixing conventional cross-correlation techniques and eventually exploiting the overlap areas [3]. In the case modeling is possible, e.g., earthquakes, the model will allow the reduction of fringes, easing the phase unwrapping. Iterative approaches will improve the retrieval of the true deformation. Section 3.4 shows an example in a glacier scenario, where the approach presented in [4] is used.

3. SENTINEL-1 RESULTS

This section shows several results that demonstrate the excellent interferometric capabilities of Sentinel-1, both in terms of quality and coverage. Section 3.1 shows a quantitative analysis of some InSAR relevant parameters. Since the last change in the synchronization strategy on October 3rd, 2014, Sentinel-1 has been building up stacks very fast thanks to the 12 day repeat-pass. First time series results were presented at the InSARap [5] and Fringe [6] workshops by different independent groups. Sections 3.2 and 3.3 show the time series results over the pilot sites of Campi Flegrei and Mexico City, while Section 3.4 shows some preliminary results over Greenland glaciers as an example of a scene with large azimuthal displacements.

3.1. Sentinel-1 Interferometric Performance

Fig. 2 shows the Sentinel-1 performance in terms of burst misynchronization, Doppler centroid and perpendicular baseline, based on the analysis of more than 100 interferograms. The standard deviations (1-sigma) for the burst synchronization, the Doppler centroid and the perpendicular baseline are 1.8 ms, 20Hz and 75 m, respectively. The common azimuth bandwidth is larger than 95% of the total azimuth bandwidth, while the range spectral shift is negligible due to the small orbital tube. These numbers confirm the excellent orbit and attitude control of Sentinel-1 for achieving an excellent interferometric performance [7].

3.2. Campi Flegrei Time Series

The time series over the Campi Flegrei/Vesuvius pilot site (Italy) has been analyzed. It is composed of 13 images acquired between October 14th, 2014 and April 24th, 2015. During this period, the Campi Flegrei area was experiencing an uplift of about 0.5 cm/month, as well as a horizontal displacement. The displacement pattern can be observed in the retrieved mean deformation velocity maps of Fig. 3. The time series were also validated with GPS measurements obtained over the continuous GPS stations that INGV maintains around the area [9]. Fig. 4 shows the result of the comparison

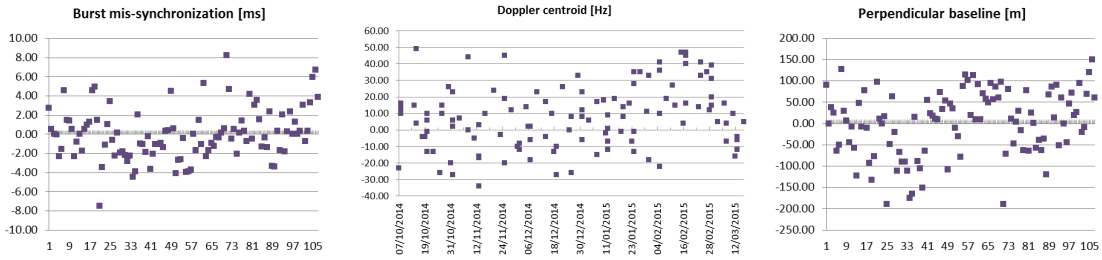

Fig. 2. Quantitative analysis of the Sentinel-1 InSAR performance in terms of burst synchronisation, Doppler centroid and baseline.

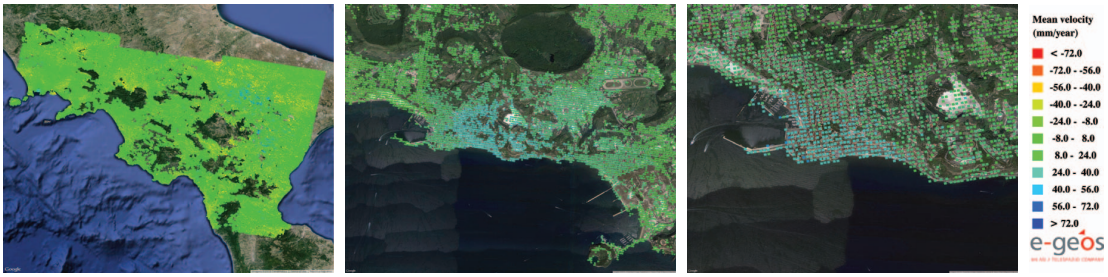

Fig. 3. Mean deformation velocity obtained with the e-GEOS' PSP-IFSAR processor [8]. The images correspond to: the complete slice of the descending acquisition; a zoom of it on the Campi Flegrei caldera, where the uplift can be observed; and a second zoom over the same area for the ascending acquisition.

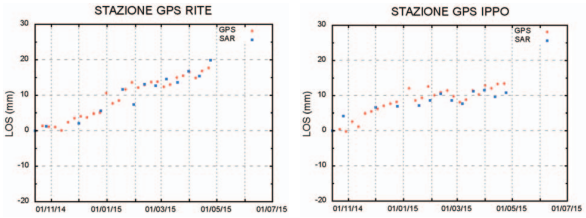

Fig. 4. PSI time series compared to GPS measurements for two different continuous GPS stations.

for two continuous GPS (cGPS) stations close to the area of maximum deformation. The agreement between GPS measurements and SAR data is very good in spite of the reduced number of SAR images. It is worth remarking that no artifacts can be observed between burst or sub-swaths, hence confirming the TOPS InSAR processing was properly done.

3.3. Mexico City Time Series

The second times series analysis focuses on Mexico City, where a well-known subsidence pattern is present due to ground water extraction. Thanks to the large swath, there are four Sentinel-1 tracks available that cover Mexico City or most of it. This data set offers an excellent opportunity to validate the implemented InSAR and PSI chain for TOPS

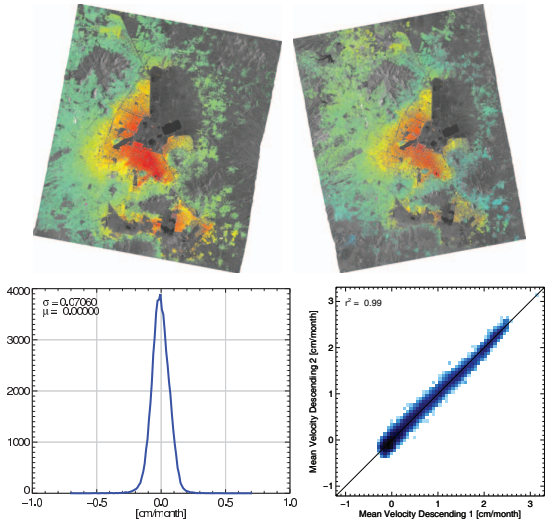

Fig. 5. Estimated mean deformation velocity over Mexico City for the (top left) descending and (top right) ascending configurations. Comparison of the retrieved mean deformation velocity between the two descending configurations: (bottom left) 1D and (bottom right) 2D histograms. InSAR and PSI processing performed with DLR-HR's TAXI processor.

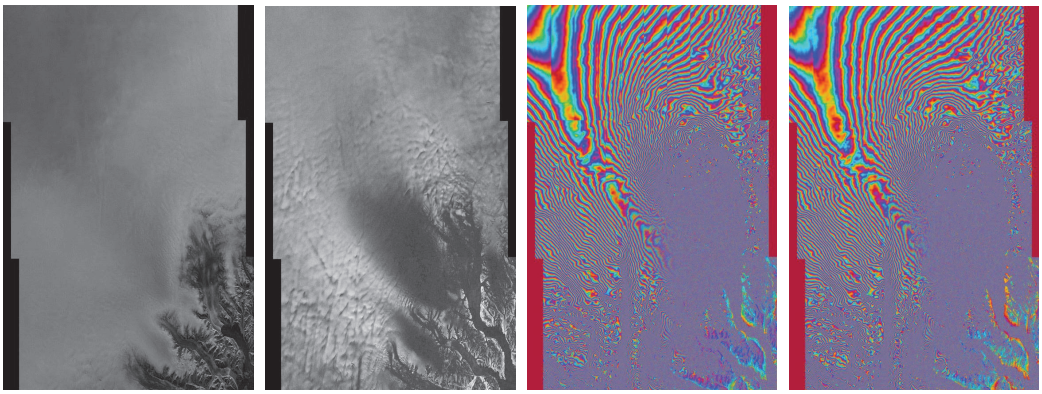

Fig. 6. Interferometric results over a Greenland glacier. The images correspond to the reflectivity image, the coherence image, the original phase, and the final phase after the processing suggested in [4]. The phase jumps between bursts in the last image have disappeared almost everywhere. Radar illumination from the top.

data. Fig. 5 shows the retrieved mean deformation velocity map around Mexico City for the ascending and descending configurations. In order to evaluate the quality of the InSAR and PSI processing, the results of the different geometries were compared. In order to do so, the line-of-sight deformation was projected to the local vertical component, i.e., it was assumed that the deformation was mainly subsidence. Fig. 5 also shows the comparison of the estimated mean deformation velocity between the two descending configurations, which show the best performance due to the reduced amount of atmospheric artifacts (descending acquisitions occur at dawn). The standard deviation of the difference is 0.05 cm/month (6 mm/year) with a total of 17 images and a time span of 6 months, hence resulting again in a very good performance. Similar as in the previous section, no unexpected artifacts could be observed.

3.4. Glaciers

The last example represents a more challenging scenario. The data takes were acquired over Greenland, where the glacier motion is clearly sensed by the variable LOS of the TOPS mode, hence introducing clear phase jumps between bursts. The displacement is so large in some areas that the phase jumps can be larger than $\pm\pi$. Fig. 6 shows the interferogram under investigation. The first phase image shows clear jumps, especially in the first sub-swath. In order to mitigate the phase jumps and allow for a proper exploitation of the differential phase, the methodology proposed in [4] has been applied. It consists in a first estimation of the motion using conventional speckle tracking, followed by a second refinement by applying spectral diversity (SD) within the processed bandwidth. After coregistering the slave image using the estimated shifts (both in the range and azimuth dimensions) most of the phase jumps disappear, hence proving that the azimuthal component of the motion could be properly estimated.

4. CONCLUSION

This paper has presented some first Sentinel-1 interferometric results. In the first part of the paper the methodology to obtain reliable InSAR TOPS products has been briefly described, putting special emphasis on the varying line of sight. In the second part of the paper several Sentinel-1 results have been shown. These results include a quantitative analysis of relevant parameters for InSAR performance, time series results over Campi Flegrei (validated with GPS measurements) and Mexico City (cross-validation with different geometries), and very promising results over a glacier scenario. All these results confirm the excellent capabilities of the IW mode for interferometric applications.

5. REFERENCES

[1] R. Torres, P. Snoeij, D. Geudtner, D. Bibby, M. Davidson, E. Attema, P. Potin, et al., "GMES Sentinel-1 mission," *Remote Sensing of Environment*, vol. 120, pp. 9–24, 2012.

[2] P. Prats, R. Scheiber, L. Marotti, S. Wollstadt, and A. Reigber, "TOPS interferometry with TerraSAR-X," *IEEE Trans. Geosci. Remote Sens.*, vol. 50, no. 8, pp. 3179–3188, Aug. 2012.

[3] F. De Zan, P. Prats-Iraola, R. Scheiber, and A. Rucci, "Interferometry with TOPS: coregistration and azimuth shifts," in *Proceedings of EUSAR*, 2014.

[4] R. Scheiber, M. Jaeger, P. Prats-Iraola, F. De Zan, and D. Geudtner, "Speckle tracking and interferometric processing of TerraSAR-X TOPS data for mapping nonstationary scenarios," *IEEE JSTARS*, 2014, to be published.

[5] "InSARap workshop," 2014, http://seom.esa.int/insarap/.

[6] "Fringe workshop," 2015, http://seom.esa.int/fringe2015/.

[7] P. Prats-Iraola, M. Rodriguez-Cassola, F. De Zan, R. Scheiber, P. Lopez-Dekker, I. Barat, and D. Geudtner, "Role of the orbital tube in interferometric spaceborne SAR missions," *IEEE Geosci. Remote Sens. Lett.*, 2015, to be published.

[8] M. Costantini, S. Falco, F. Malvarosa, F. Minati, F. Trillo, and F. Vecchioli, "Persistent scatterer pair interferometry: Approach and application to COSMO-SkyMed SAR data," *Selected Topics in Applied Earth Observations and Remote Sensing, IEEE Journal of*, vol. 7, no. 7, pp. 2869–2879, 2014.

[9] P. De Martino, U. Tammaro, and F. Obrizzo, "GPS time series at Campi Flegrei caldera (2000-2013)," *Annals of Geophysics*, vol. 57, no. 2, 2014.